Fabrice Dal Bo*, Sergey M. Aksenov, Frédéric Hatert and Peter C. Burns

Synthesis, IR spectroscopy and crystal structure of [(UO$_2$)$_2${Be(H$_2$O)$_2$(PO$_4$)$_2$}]·(H$_2$O), the first compound with a trimer beryllophosphate anion

Abstract: The first uranyl beryllophosphate, [(UO$_2$)$_2${Be(H$_2$O)$_2$(PO$_4$)$_2$}]·(H$_2$O), has been synthesized under hydrothermal conditions at 200 °C. The monoclinic unit-cell parameters are: $a = 9.3361(1)$, $b = 8.8545(4)$, $c = 9.6592(10)$ Å, $\beta = 93.211(1)°$, $V = 797.21(6)$ Å^3, space group $P2/n$, $Z = 2$. The crystal structure has been solved by direct methods and refined to final $R_1 = 4.92\%$ using 1294 $I > 3\sigma(I)$ reflections in the anisotropic approximation. The structure consists of sheets of UrO$_5$ pentagonal bipyramids and PO$_4$ tetrahedra. UrO$_5$ bipyramids are linked by edge-sharing to form infinite chains. Adjacent chains of UrO$_5$ bipyramids are connected by sharing alternating edges of uranyl bipyramids with PO$_4$ tetrahedra. The resulting sheets are based on the well-known uranophane anion-topology. Be atoms are tetrahedrally coordinated by two oxygen atoms of PO$_4$ tetrahedra and two water molecules in the interlayer space. One isolated water molecule also occurs in the interlayer space, where it is held in position by H bonds. The connection between the phosphorus and beryllium tetrahedra leads to formation of an unbranched trimer [BeP$_2$O$_8$(H$_2$O)$_2$]$^{4-}$ observed for the first time in inorganic oxysalts.

Keywords: beryllophosphate; hydrothermal synthesis; single-crystal X-ray analysis; uranophane-anion topology; uranyl ion.

*Corresponding author: Dr. Fabrice Dal Bo, Laboratory of Mineralogy, University of Liège, B-4000 Liège, Belgium; and Department of Civil and Environmental Engineering and Earth Sciences, University of Notre Dame, Notre Dame, IN 46556, USA, E-mail: fabrice.dalbo@gmail.com
Sergey M. Aksenov: Department of Civil and Environmental Engineering and Earth Sciences, University of Notre Dame, Notre Dame, IN 46556, USA
Frédéric Hatert: Laboratory of Mineralogy, University of Liège, B-4000 Liège, Belgium
Peter C. Burns: Department of Civil and Environmental Engineering and Earth Sciences, University of Notre Dame, Notre Dame, IN 46556, USA; and Department of Chemistry and Biochemistry, University of Notre Dame, Notre Dame, IN 46556, USA

Introduction

Recent research in nuclear fuel cycle technologies has shown that uranium-beryllium fuel has potentially useful properties. The insertion of Be in nuclear fuel rods may provide a better performance in the reactor by increasing the thermal conductivity of the fuel, by decreasing the internal pressure and the release of fission gas [1–4]. Uranium and beryllium are highly toxic and their recovery from spent nuclear fuel is important. Consequently, in order to develop new management techniques for such nuclear waste, it is important to increase our chemical and structural knowledge of the compounds containing both U and Be.

To date, more than 230 mineral species containing uranium as a major component are known. However, despite this huge number of U mineral species and the increasing interest for U mineralogy, no minerals containing both U and Be and reported in the literature [5, 6], no doubt due to the lack of geochemical environments that feature these two elements. Considering synthetic compounds, very few compounds containing both U and Be are reported: one alloy, UBe$_{13}$ [7]; three oxysalt compounds, Ba$_2$BeUO$_6$ [8], Be(UO$_2$)(SO$_4$)$_2$(H$_2$O)$_8$ [9] and Be(UO$_2$)$_3$(SeO$_4$)$_4$(H$_2$O)$_{22}$ [10]; and one fluoride compound, NaBeU$_3$F$_{15}$ [11]. Unfortunately the crystal structures are only known for the compound Ba$_2$BeUO$_6$ and UBe$_{13}$. Note that several studies [12–14] have shown that UBe$_{13}$ has interesting superconductivity properties at very low temperatures.

In this paper, we report the hydrothermal synthesis, single crystal X-ray structure analysis and IR spectra of the first uranyl beryllium phosphate, [(UO$_2$)$_2${Be(H$_2$O)$_2$(PO$_4$)$_2$}]·(H$_2$O), and we describe in detail its crystal structure as well as its relationships to related compounds.

Experimental

Synthesis

Single crystals of [(UO$_2$)$_2${Be(H$_2$O)$_2$(PO$_4$)$_2$}]·(H$_2$O) were synthesized under hydrothermal conditions at 200 °C. The following

analytical-grade compounds were used: BeO, $UO_2(CH_3COO)_2 \cdot 2H_2O$ and H_3PO_4. The synthesis was carried out with the BeO:UO_3:P_2O_5 molar ratio 2:1:2. A mixture of the reactants including 2 mL of ultra-pure water was heated in a Parr 23-mL autoclave with PTFE liner. After 5 days at 200 °C, the autoclave was slowly cooled to 100 °C (1.5 °C/h) and then cooled to room temperature by switching off the furnace. The resulting products were recovered by filtration and washed with distilled water, and only contained yellow, transparent and platy crystals of the title compound.

IR spectroscopy

The infrared spectrum of the title compound was recorded using a Nicolet NEXUS spectrometer over the 400–4000 cm^{-1} region. The sample was prepared by intimately mixing 2 mg of sample with KBr, in order to obtain a 150 mg homogenous pellet. To prevent water contamination the measurements were performed under a dry air purge. The IR spectra of $[(UO_2)_2\{Be(H_2O)_2(PO_4)_2\}]\cdot(H_2O)$ is shown in Figure 1, and the assignment of the absorption bands is given in Table 1.
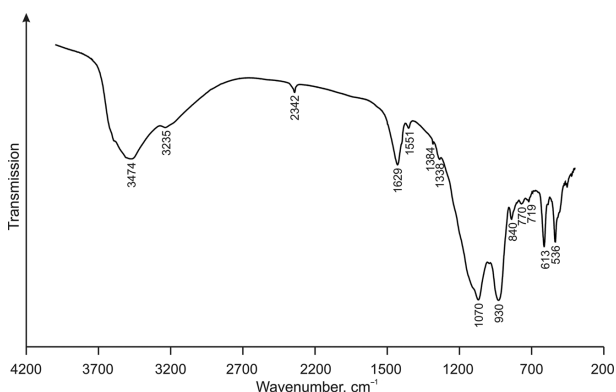
Fig. 1: The IR spectra of $[(UO_2)_2\{Be(H_2O)_2(PO_4)_2\}]\cdot(H_2O)$.

Tab. 1: Assignment of the infrared absorption bands (cm^{-1}) for $[(UO_2)_2\{Be(H_2O)_2(PO_4)_2\}]\cdot(H_2O)$.

Band (cm^{-1})	Description
3474	O–H-stretching vibrations (H-bond of a medium strength)
3235	O–H-stretching vibrations (strong H-bond)
2342	CO_2 molecules entrapped in the structure (low amounts)
1629	H–O–H bending vibrations (H-bond of a medium strength)
1551	H–O–H bending vibrations (strong H-bond)
1338–1384	Ambiguous assignment
1070	ν_3 asymmetric stretching vibrations of PO_4
930	Asymmetric stretching vibrations of the uranyl ion $(UO_2)^{2+}$
840	Vibrations of H_2O molecules forming strong H-bonds
719–770	ν_4 Be–O-stretching vibrations
536–613	ν_4 Bending vibrations of PO_4
Below 536	Mixed lattice modes

Single-crystal X-ray analysis

The X-ray structural study of the title compound was carried out on an Oxford Diffraction Xcalibur four-circle diffractometer (kappa geometry), using MoKα radiation ($\lambda = 0.71073$ Å, 40 kV, 40 mA), and equipped with an EOS CCD area detector, on a crystal fragment measuring 0.22 mm × 0.11 mm × 0.04 mm. The data were corrected for Lorentz, polarization and absorption effects, with the latter done using an empirical method in the SCALE3 ABSPACK scaling algorithm included in the CrysAlisRED package [15]. A total of 3955 reflections within the sphere limited by $\theta = 29.03°$ were measured. Experimental details of the data collection and refinement results are listed in Table 2. The unit-cell parameters were obtained by the least-squares refinement: $a = 9.3361(1)$ Å, $b = 8.8545(4)$ Å, $c = 9.6592(10)$ Å, $\beta = 93.221(1)°$,

Tab. 2: Crystal data, data collection and refinement of $[(UO_2)_2\{Be(H_2O)_2(PO_4)_2\}]\cdot(H_2O)$.

Crystal data	
Formula	$[(UO_2)_2\{Be(H_2O)_2(PO_4)_2\}]\cdot(H_2O)$
Formula weight (g)	787
Temperature (K)	293
Cell setting	Monoclinic
Space group	$P2/n$ (No. 13)
Lattice parameters	
a (Å)	9.3361(3)
b (Å)	8.8545(4)
c (Å)	9.6592(10)
β (°)	93.221(1)
V (Å^3)	797.21(6)
Z	2
Calculated density, Dx (g·cm^{-3})	3.2785
Crystal size (mm)	0.22 × 0.11 × 0.04
Crystal form	Plate crystal
Crystal color	Yellow
Data collection	
Diffractometer	Xcalibur Oxford Diffraction (CCD-detector)
Radiation; λ	MoK$_\alpha$; 0.71073
Absorption coefficient, μ (mm^{-1})	20.552
$F(000)$	688
Data range θ (°); h, k, l	2.30–29.03; $-12 < h < 8$, $-12 < k < 10$, $-10 < l < 12$
No. of measured reflections	3955
Total reflections (N_{tot})/unique(N_{ref})	1852/1294
Criterion for observed reflections	$I > 3\sigma(I)$
Refinement	
Refinement on	Full-matrix least squares on F
R_1, wR_1 ($F > 4\sigma(F)$)	4.92/6.08
R_2, wR_2 (all reflection)	7.29/6.95
R_{int} (%)	7.08
No. of refinement parameters (N_{par})	96
N_{ref}/N_{par}	13.49
Weight scheme	$1/(\sigma^2|F| + 0.002025F^2)$
Min./max. residual e density, (eÅ^{-3})	-1.57 /2.24
GOF (Goodness of fit)	1.01

$R_1 = \sum ||F_{obs}| - |F_{calc}|| / \sum |F_{obs}|$; $wR_2 = \{\sum[w(F_{obs}^2 - F_{calc}^2)^2]/\sum[w(F_{obs}^2)^2]\}^{1/2}$; GOF $= \{\sum[w(F_{obs}^2 - F_{calc}^2)]/(n-p)\}^{1/2}$ where n is a number of reflections and p is a number of refined parameters.

$V = 797.21(6)$ Å^3. The centrosymmetric monoclinic space group $P2/n$ was chosen.

A structural model was determined by the "charge flipping" method using the SUPERFLIP program [16]. The structure determination and refinement were carried out using the Jana2006 program package [17]. Scattering curves for neutral atoms and anomalous dispersion corrections were taken from the *International Tables for Crystallography* [18]. Illustrations were produced with the JANA2006 program package in combination with the program VESTA 3 [19] and Diamond 3 [20].

The final refinement cycles converged with $R_1 = 4.92\%$, w$R_2 = 6.95\%$, GOF = 1.01 for 1294 $I > 3\sigma(I)$. The highest peak and deepest minimum in the final residual electron density map were 2.24 eÅ^{-3} and –1.57 eÅ^{-3}, and they are both close to the U-site. Table 3 lists the fractional atomic coordinates, occupancy, site symmetry and equivalent atomic displacement parameters (U_{eq}). Anisotropic atomic displacement parameters (U_{ij}) are presented in Table 4. Selected interatomic distances and bond angles are given in Table 5.

The bond-valence sums (BVS) have been calculated for the atoms located in the structure, according to the parameters for P^{5+}–O and Be^{2+}–O bonds [21], as well as for U^{6+}–O bond [22]. The calculated BVS are 4.98, 2.06 and 6.02 for P, Be and U, respectively (Table 6). The BVS for the oxygen atoms belonging to the uranyl-phosphate sheets

Tab. 3: Fractional atomic coordinates, site symmetry, and equivalent atomic displacement parameters (U_{eq}, Å^2) for [(UO$_2$)$_2$\{Be(H$_2$O)$_2$(PO$_4$)$_2$\}]·(H$_2$O).

Atom	x	y	z	Site	U_{eq}
U	0.79739(4)	0.95814(5)	0.05161(5)	4g	0.0249(2)
P	0.0506(3)	0.9121(4)	0.2806(3)	4g	0.0265(9)
Be	0.25	0.664(4)	0.25	2e	0.048(10)
O1	0.7773(10)	0.1486(11)	0.0920(11)	4g	0.037(3)
O2	0.8178(10)	0.7630(13)	0.0140(11)	4g	0.043(3)
O3	0.6128(8)	0.9021(12)	0.2016(9)	4g	0.032(3)
O4	0.6190(10)	0.9708(9)	–0.1211(11)	4g	0.031(3)
O5	0.1190(9)	0.7595(12)	0.2995(11)	4g	0.043(3)
O6	0.9468(9)	0.0328(11)	–0.1283(9)	4g	0.032(3)
W1	0.2987(19)	0.5520(19)	0.375(2)	4g	0.125(9)
W2[a]	0.523(3)	0.662(3)	–0.215(5)	4g	0.109(16)

U_{eq} is defined as one third of the trace of the orthogonalized U_{ij} tensor.
[a]The occupancy factor of the W2 site was constrained to 0.5.

Tab. 5: Selected interatomic distances (Å) and angles (°) in the structure of [(UO$_2$)$_2$\{Be(H$_2$O)$_2$(PO$_4$)$_2$\}]·(H$_2$O).

Bond	d, Å	Bond	d, Å	Angle	°
U–O1	1.785(13)	P–O3	1.509(10)	O3–P–O4	110.6(5)
U–O2	1.746(12)	P–O4	1.556(19)	O3–P–O5	110.5(6)
U–O3	2.311(11)	P–O5	1.517(15)	O3–P–O6	101.0(5)
U–O4	2.365(17)	P–O6	1.561(12)	O4–P–O5	112.1(6)
U–O4	2.526(8)	<P–O>	1.53	O4–P–O6	110.4(6)
U–O6	2.369(17)			O5–P–O6	111.7(6)
U–O6	2.469(15)	Be–O5	1.57(3)×2		
<U–O$_{Ur}$>	1.76	Be–W1	1.69(3)×2	O5–Be–O5	115.4(5)
<U–O$_{eq}$>	2.41	<Be–O>	1.63	O5–Be–W1	107.1(7)
				O5–Be–W1	111.4(7)
W1–O2	3.10(2)	W2–O4	3.00(3)	W1–Be–W1	103.9(9)
W1–W2	3.01(4)	W2–O1	3.33(4)		

Tab. 6: Bond valence calculation for [(UO$_2$)$_2$\{Be(H$_2$O)$_2$(PO$_4$)$_2$\}]·(H$_2$O).

Atom	U	P	Be	$\sum_v a$
O1	1.67			1.67
O2	1.80			1.80
O3	0.61	1.33		1.94
O4	0.55	1.18		2.13
	0.40			
O5		1.31	0.60×2↓	1.91
O6	0.45	1.16		2.15
	0.54			
W1			0.43×2↓	0.43
W2[a]				–
$\sum_v c$	6.02	4.98	2.06	

[a]Water molecule that does not have short contacts with cations.
$\sum_v a$ and $\sum_v c$ are the bond valence sums for anions and cations, respectively.
The ×2↓ sign indicates the doubling of the corresponding valence contributions in columns due to symmetry.

(O1–O6) vary between 1.67 and 2.15. The BVS for the W1 atom, which is only connected to the Be atom, is 0.43. These BVS values confirm the cationic distribution, as well as the presence of water molecules at the W1 and W2 sites.

Tab. 4: Anisotropic atomic displacement parameters (U_{ij}, Å^2) for [(UO$_2$)$_2$\{Be(H$_2$O)$_2$(PO$_4$)$_2$\}]·(H$_2$O).

Site	U^{11}	U^{22}	U^{33}	U^{12}	U^{13}	U^{23}
U	0.0134(3)	0.0419(3)	0.0196(3)	–0.00065(19)	0.00067(18)	0.0002(2)
P	0.0119(14)	0.0490(19)	0.0185(15)	0.0013(13)	–0.0001(11)	–0.0003(14)
Be	0.032(14)	0.0057(18)	0.06(2)	0	0.018(13)	0
O1	0.037(5)	0.039(5)	0.036(5)	0.003(4)	0.004(4)	0.001(4)
O2	0.035(5)	0.058(6)	0.037(6)	0.015(5)	0.000(4)	–0.016(5)
O3	0.009(4)	0.055(6)	0.033(5)	0.000(4)	–0.001(3)	–0.002(4)
O4	0.019(5)	0.037(5)	0.035(6)	–0.002(4)	–0.003(4)	0.006(4)
O5	0.022(4)	0.053(6)	0.053(7)	0.005(5)	–0.001(4)	–0.003(5)
O6	0.018(4)	0.063(7)	0.015(4)	–0.002(4)	0.001(3)	0.002(4)
W1	0.089(13)	0.114(14)	0.18(2)	–0.063(10)	0.067(13)	0.099(13)
W2	0.09(2)	0.026(11)	0.21(4)	0.018(13)	0.02(2)	–0.018(18)

Results

IR spectroscopy

According to the fundamental vibrational frequencies of the PO$_4$ tetrahedron [23], the absorption band at 1070 cm^{-1} can be attributed to the antisymmetric stretching mode (v_3), and the bands between 536 and 613 cm^{-1} to the bending mode (v_4) of the PO$_4$ anions. The band at 930 cm^{-1} is attributed to the antisymmetric stretching vibration (v_3) of the uranyl ion (UO$_2$)$^{2+}$, and is in agreement with the values reported for uranyl minerals [24]. The bands in the 719–770 cm^{-1} region are assigned to the stretching vibrations (v_4) of the BeO$_4$ tetrahedra, by analogy to the IR spectra of beryllophosphate minerals. However, these bands have anomalously low intensities that may indicate a low electric dipole moment of the Be−O bond. Bands in the 3235–3474, 1551–1629 and 840 cm^{-1} regions are attributed to O−H and H−O−H stretching vibrations modes, consistent with the water content of the title compound. The 2342 cm^{-1} band, which has a high extinction coefficient, is attributed to CO$_2$ molecules entrapped in the structure in very low amount.

Crystal structure

The layered crystal structure of the novel compound [(UO$_2$)$_2$\{Be(H$_2$O)$_2$(PO$_4$)$_2$\}]·(H$_2$O) is composed of sheets of uranyl, beryllium and phosphate polyhedra (Figure 2).

U^{6+} cations form typical nearly linear (UO$_2$)$^{2+}$ uranyl ions (designed *Ur*). (UO$_2$)$^{2+}$ uranyl ions are coordinated by five O atoms arranged at the equatorial vertices of *Ur*O$_5$ pentagonal bipyramids. The mean <U−O$_{eq}$> (O$_{eq}$: equatorial O atom) bond length is 2.41 Å and the mean <U−O$_{Ur}$> (O$_{Ur}$: apical O atom) bond length is 1.76 Å. These values are in good agreement with the average values of 2.37(9) Å (<U−O$_{eq}$>) and 1.79(4) Å (<U−O$_{Ur}$>) generally reported for *Ur*O$_5$ pentagonal bipyramids [25, 26]. The uranyl pentagonal bipyramids share common edges forming parallel infinite chains going along [101].

Adjacent chains are connected via PO$_4$-tetrahedra (<P−O>=1.53 Å), forming a heteropolyhedral uranyl-phosphate [(UO$_2$)$_2$(PO$_4$)$_2$]$^{2-}$ sheet. The P^{5+} cation is coordinated by three equatorial oxygen atoms of *Ur*O$_5$ pentagonal bipyramids and one apical O5 oxygen directed into the interlayer space. The negative charge of the sheet structural unit is compensated by Be^{2+} cations occurring in a distorted [Beϕ_4]-tetrahedron linked with two [PO$_4$]-tetrahedra via O5 bridging oxygens [Be−O5=1.57(3) Å]. The
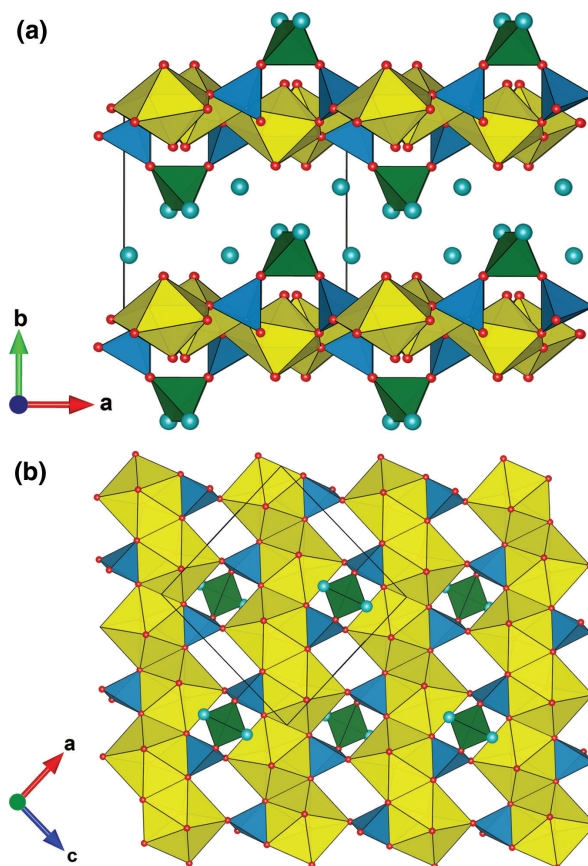
Fig. 2: The general view of the crystal structure of [(UO$_2$)$_2$\{Be(H$_2$O)$_2$(PO$_4$)$_2$\}]·(H$_2$O) (a) and heteropolyhedral sheet (b). *Ur*O$_5$ polyhedra = yellow, PO$_4$ tetrahedra = blue, BeO$_2$(H$_2$O)$_2$ tetrahedra = green. Oxygen atoms and water molecules are shown as red and cyan circles, respectively.

Be atom is also coordinated by two *W*1 water molecules in the interlayer space [Be−*W*1=1.69(3) Å], thus forming [BeO$_2$(H$_2$O)$_2$] tetrahedra, which are positioned on both
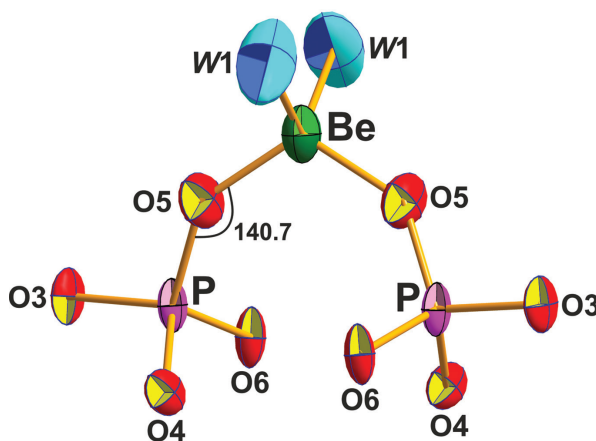
Fig. 3: [BeP$_2\phi_{10}$]$^{n-}$-trimer in the crystal structure of [(UO$_2$)$_2$\{Be(H$_2$O)$_2$(PO$_4$)$_2$\}]·(H$_2$O).

sides of the uranyl phosphate sheets. The connection between the phosphorus and beryllium tetrahedra lead to the formation of an unbranched trimer [BeP$_2$O$_8$(H$_2$O)$_2$]$^{4-}$ observed here for the first time in inorganic oxysalts (Figure 3).

Adjacent mixed uranyl beryllium-phosphate layers are linked by weak hydrogen bonds of W1 water molecules of the [Beϕ_4]-tetrahedron and isolated W2 water molecules that occupy the interlayer space (Table 5).

Discussion

Anion topology and stereoisomerism

Following the method of Burns et al. [26], the anion-type topology of the uranyl-phosphate [(UO$_2$)$_2$(PO$_4$)$_2$] sheets of the studied compound are represented by pentagons (**P**), triangles (**T**), and squares (**S**) (Figure 4a), and belongs to uranophane-type topology.

The uranophane-type topology is observed in 27 inorganic uranyl compounds [26] that can be divided into several stereoisomers, depending on the orientation of the tetrahedra relative to the plane of the sheet [6]. As proposed by Burns et al. [26] and Kubatko and Burns [27], the uranophane anion topology may also be described as arrowhead chains occupied by UrO$_5$ pentagonal bipyramids and PO$_4$-tetrahedra (**PT** chains), perpendicular to chains of squares and PO$_4$ polyhedra (**ST** chains). Going along the **ST** chains, the PO$_4$ tetrahedra either point downward (**D**) or upward (**U**). The observed sequence is **DDUUDD** (Figure 4b), leading to the formation of squares with adjacent PO$_4$ tetrahedra pointing in the same direction. In these specific squares, apical O6 oxygen atoms of the two adjacent PO$_4$ tetrahedra are close enough to each other to allow the connection of [Beϕ_4] tetrahedra (Figure 2b).

Along the **PT** chains the orientation of the PO$_4$ tetrahedra follows the **UDUD** sequence, with a perfect alternation in the orientation of the PO$_4$ tetrahedra (Figure 4b). The sequence in the **ST** chains is the same as that observed in β-uranophane [28] and several other synthetic uranyl phosphates and arsenates [28–31]. However, the (**DUDU**)-sequence in the **PT** chains is not observed in β-uranophane. Only the mineral oursinite [27] shows the **DUDU** sequence in the **PT** chains, as well as several synthetic uranyl oxysalts [29–32]. To conclude, [(UO$_2$)$_2${Be(H$_2$O)$_2$(PO$_4$)$_2$}]·(H$_2$O) shows the same geometrical isomer of layers as in the compounds Cs(UO$_2$)[(UO$_2$)(AsO$_4$)]$_3$(H$_2$O)$_5$ [29], {NHEt_3}[(UO$_2$)$_2$(PO$_4$)(HPO$_4$)] [30], and {(C$_2$H$_5$)$_2$NH$_2$}$_2$[(UO$_2$)$_5$(PO$_4$)$_4$] [31].

(a)

(b)
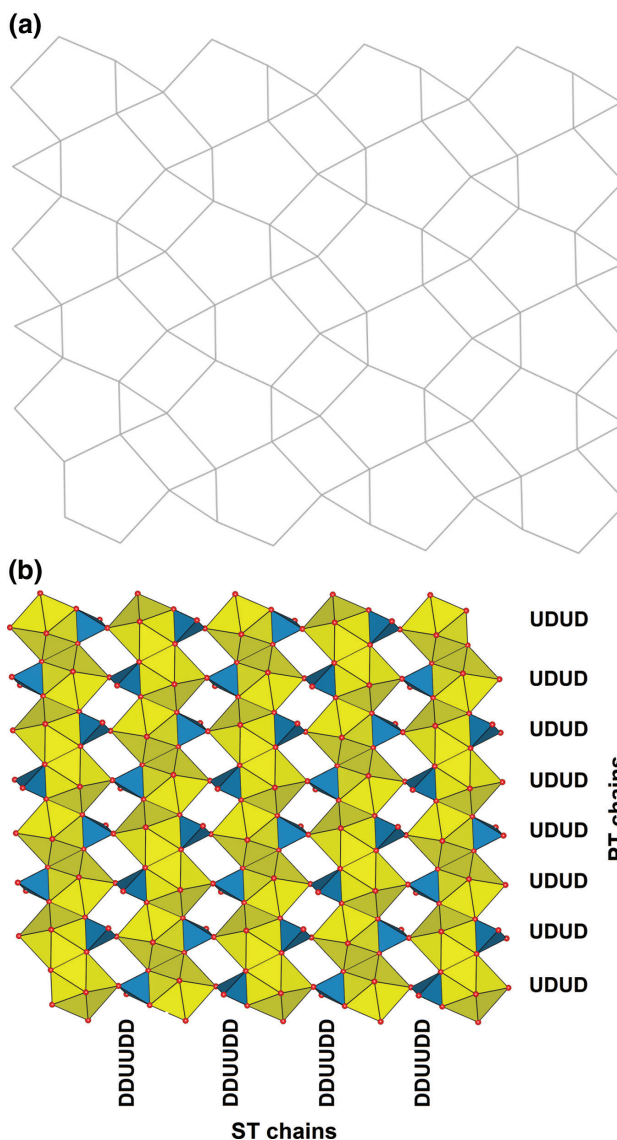
Fig. 4: Anion-topology of the [(UO$_2$)(PO$_4$)]$^-$ sheet (following the method of Burns et al. [26]) (a), and view of the tetrahedra orientation along the **ST** and **PT** chains (b).

Connectivity between [PO$_4$] and [Beϕ_4] tetrahedra

Beryllium phosphates are well known. More than 85 minerals as well as synthetic compounds have been studied by X-ray analysis. Their crystal chemical features were recently reviewed [33, 34]. In the structures of minerals, the Be^{2+} cation is tetrahedrally coordinated by oxygens and/or hydroxyl groups (typical mean Be$-\phi$ distance is 1.633 Å) [33]. In the structure of [(UO$_2$)$_2${Be(H$_2$O)$_2$(PO$_4$)$_2$}·(H$_2$O), beryllium is coordinated by two oxygen atoms and two water molecules (Figure 3), which is a very unusual environment. Among beryllium phosphates, such a

coordination is observed in the open-framework zeolite-like structure of Be$_3$(PO$_4$)$_2$·2(H$_2$O) [35], where hydrated [BeO$_2$(H$_2$O)]$^{2-}$ tetrahedra (Figure 5a) take part in the linkage of mixed beryllium phosphate layers (Figure 5b). Distances between Be^{2+} cations and apical water molecules in the structures of [(UO$_2$)$_2${Be(H$_2$O)$_2$(PO$_4$)$_2$]·(H$_2$O) and Be$_3$(PO$_4$)$_2$·2(H$_2$O) (1.69 and 1.67 Å, respectively) are in a good agreement with theoretical values (~1.66 Å) predicted by *ab initio* calculations for stable beryllium(II) aqua complex [Be(H$_2$O)$_4$]$^{2+}$ [36, 37].

It was shown that [Beϕ_4]- and [Pϕ_4]-tetrahedra are commonly linked to form infinite polyanions. With the exception of the title compound, only minerals belonging to the gainesite group (gainesite, Na(Na,K)(Be,Li)Zr$_2$(PO$_4$)$_4$·1.5-2H$_2$O [38], mccrillisite, NaCs(Be,Li)Zr$_2$(PO$_4$)$_4$·1-2H$_2$O [39], and selwynite, NaK(Be,Al)Zr$_2$(PO$_4$)$_4$·2H$_2$O [40]) are characterized by finite beryllium-phosphate anions, represented by pentameric [BeP$_4$O$_{16}$]$^{10-}$ clusters (Figure 6a), that are topologically identical to the [Si$_5$O$_{16}$]$^{12-}$ pentamers in the structure of zunyite, Al$_{13}$O$_4$[Si$_5$O$_{16}$](OH,F)$_{18}$Cl [41]. However, in the structure of

(a)

(b)

Fig. 6: Pentameric [BeP$_4$O$_{16}$]$^{10-}$-cluster (a) and general view of the gainesite-type structure (b) [38].

gainesite, beryllium-phosphate clusters are half-occupied and linked *via* common faces of [PO$_4$]-tetrahedra, forming statistical double sheets layer (Figure 6b).

Conclusions

The first uranyl beryllium phosphate, [(UO$_2$)$_2${Be(H$_2$O)$_2$(PO$_4$)$_2$}]·(H$_2$O), was hydrothermally synthesized and its crystal structure was solved. The structure consists of sheets of *Ur*O$_5$ pentagonal bipyramids and PO$_4$ tetrahedra, and is characterized by an uranophane sheet anion topology. In the present case, pentagons and triangles are occupied by *Ur*O$_5$ polyhedra and PO$_4$ tetrahedra, respectively. The crystal structure is also characterized by the presence of a complex anion with idealized formula [BeP$_2\phi_{10}$]$^{n-}$ (where ϕ = O^{2-}, H$_2$O); this trimer is the second

(a)

(b)

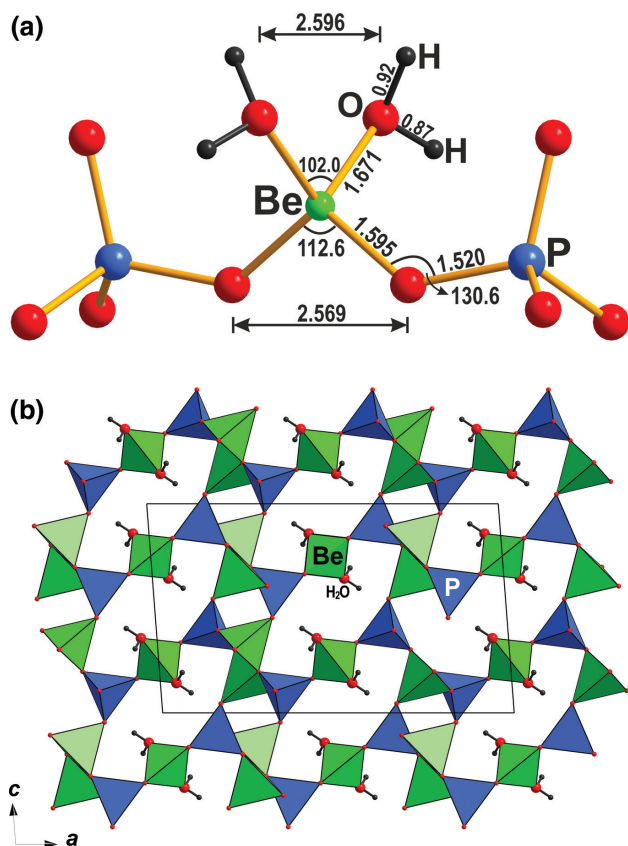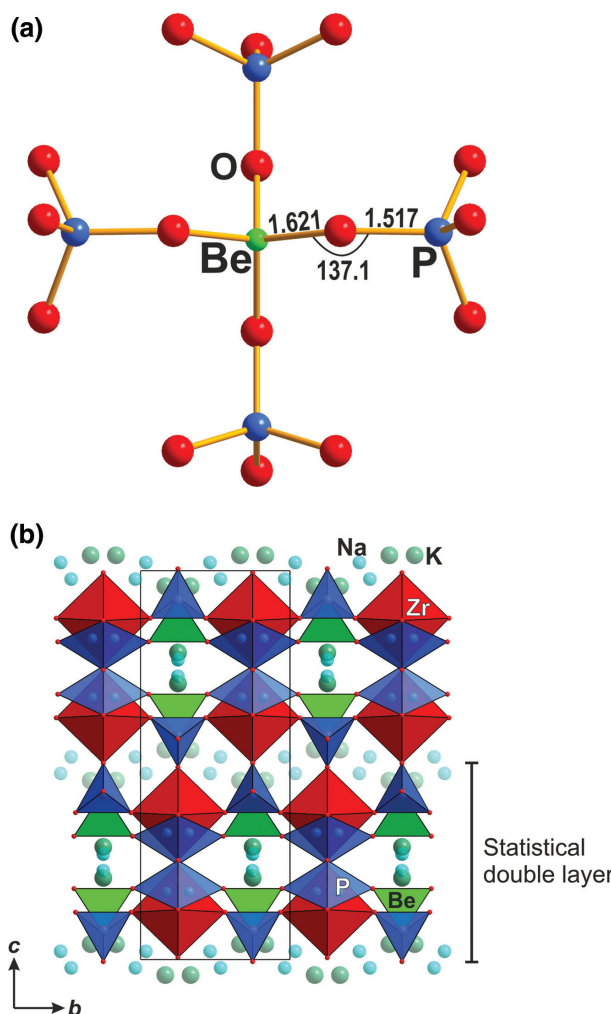**Fig. 5:** Geometry and local environment of the hydrated [BeO$_2$(H$_2$O)$_2$]$^{2-}$-tetrahedra (a) and general view of the crystal structure of Be$_3$(PO$_4$)$_2$·2(H$_2$O) [35] (b).

observation of oligomers in the structure of beryllophosphate compounds.

References

[1] K. H. Sarma, J. Fourcade, S.-G. Lee, A. A. Solomon, New processing methods to produce silicon carbide and beryllium oxide inert matrix and enhanced thermal conductivity oxide fuels. *J. Nucl. Mater*. **2006**, *352*, 324.

[2] K. McCoy, C. Mays, Enhanced thermal conductivity oxide nuclear fuels by co-sintering with BeO: II. Fuel performance and neutronics. *J. Nucl. Mater*. **2008**, *375*, 157.

[3] S. K. Kim, W. I. Ko, H. D. Kim, S. T. Revankar, W. Zhou, D. Jo, Cost-benefit analysis of BeO-UO$_2$ nuclear fuel. *Prog. Nucl. Energy* 2010, *52*, 813.

[4] A. A. Kovalishin, V. N. Prosyolkov, V. D. Sidorenko, Y. V. Stogov, On the possibility of using uranium-beryllium oxide fuel in a VVER reactor. *Phys. At. Nucl*. **2014**, *77*, 1661.

[5] R. Finch, T. Murakami, Systematics and paragenesis of uranium minerals, in *Uranium: Mineralogy, Geochemistry and the Environment,* (Eds. P. C. Burns and R. Finch) Mineralogical Society of America, Washington DC, Vol. 38, p. 91, **1999**.

[6] S. V. Krivovichev, J. Plášil, Mineralogy and crystallography of uranium, in *Uranium, from Cradle to Grave*, (Eds. P. C. Burns and G. E. Sigmon) Mineral. Assoc. Can., Winnipeg, Vol. 43, p. 15, **2013**.

[7] W. C. Koehler, J. Singer, A. S. Coffinberry, X-ray and neutron diffraction studies of the *M*Be$_{13}$ intermetallic compounds. *Acta Crystallogr*. **1952**, *5*, 394.

[8] S. K. Awasthi, D. M. Chackraburtty, V. K. Tondon, Tetravalent, pentavalent and hexavalent uranium compounds of the type A$_2$BB'O$_6$. *J. Inorg. Nucl. Chem*. **1967**, *29*, 1225.

[9] V. Serezhkin, L. Serezhkina, Synthesis and investigation of sulfouranylberyllata. *Radiokhimiya* **1979**, *21*, 827. (in Russian)

[10] L. B. Serezhkina, Y. G. Kudryashova, V. N. Serezhkin, BeSeO$_4$–UO$_2$SeO$_4$–H$_2$O system at 25°C. *Zhurnal Neorganicheskoi Khimii*. **1983**, *28*, 1054. (in Russian)

[11] R. E. Thoma, C. F. Weaver, H. A. Friedman, L. A. Harris, The compounds NaF · BeF$_2$ · 3ThF$_4$ and NaF · BeF$_2$ · 3UF$_4$. *J. Am. Ceram. Soc*. **1960**, *43*, 608.

[12] H. R. Ott, H. Rudigier, Z. Fisk, J. L. Smith, UBe$_{13}$: An unconventional actinide superconductor. *Phys. Rev. Lett*. **1983**, *50*, 1595.

[13] N. E. Alekseevskii, V. I. Nizhankovskii, V. N. Narozhnyi, E. P. Khlybov, A. V. Mitin, Investigation of UBe$_{13}$ and other beryllium and uranium compounds in normal and superconducting states. *J. Low Temp. Phys*. **1986**, *64*, 87.

[14] F. Gross, B. S. Chandrasekhar, D. Einzel, K. Andres, P. J. Hirschfeld, H. R. Ott, J. Beuers. Z. Fisk and J. L. Smith, Anomalous temperature dependence of the magnetic field penetration depth in superconducting UBe$_{13}$. *Z. Phys. B. Condens. Matter* **1986**, *64*, 175.

[15] Agilent Technologies. CrysAlis CCD and CrysAlis RED, Oxford Diffraction Ltd., Yarnton, Oxfordshire, UK, **2012**.

[16] L. Palatinus, G. Chapuis, SUPERFLIP – a computer program for the solution of crystal structures by charge flipping in arbitrary dimensions. *J. Appl. Cryst*. **2007**, *40*, 786.

[17] V. Petříček, M. Dušek, L. Palatinus, Jana2006. Crystallographic computing system JANA2006 – General features. *Z. Kristallogr*. **2006**, *229*, 345.

[18] International Tables for Crystallography. Vol. C, Mathematical, physical and chemical Tables, **2006**.

[19] K. Momma, F. Izumi, VESTA 3 for three-dimensional visualization of crystal, volumetric and morphology data. *J. Appl. Crystallogr*. **2011**, *44*, 1272.

[20] K. Brandenburg, H. Putz. *DIAMOND, Version 3*. Crystal Impact GbR. Bonn, Germany, **2005**.

[21] I. D. Brown, D. Altermatt, Bond-valence parameters obtained from a systematic analysis of the inorganic crystal structure database. *Acta Crystallogr*. **1985**, *B41*, 244.

[22] P. C. Burns, R. C. Ewing, F. C. Hawthorne, The crystal chemistry of hexavalent uranium: polyhedron geometries, bond-valence parameters, and polymerization of polyhedra. *Can. Mineral*. **1997**, *35*, 1551.

[23] V. C. Farmer, The infrared spectra of minerals. *Mineral. Soc. Monogr*. **1974**, *4*, 539.

[24] J. Čejka, Infrared spectroscopy and thermal analysis of the uranyl minerals. *Rev. Mineral*. **1999**, *38*, 521.

[25] A. J. Luissier, R. A. K. Lopez, P.C. Burns, A revised and expanded structure hierarchy of natural and synthetic hexavalent uranium compounds. *Can. Mineral*. **2016**, *54*, 177.

[26] P. C. Burns, M. L. Miller, R. C. Ewing, U^{6+} minerals and inorganic phases: a comparison and hierarchy of crystal structures. *Can. Mineral*. **1996**, *34*, 845.

[27] K. A. Kubatko, P. C. Burns, A novel arrangement of silicate tetrahedra in the uranyl silicate sheet of oursinite, (Co$_{0.8}$Mg$_{0.2}$)[(UO$_2$)(SiO$_3$OH)]$_2$(H$_2$O)$_6$. *Am. Mineral*. **2006**, *91*, 333.

[28] K. Viswanathan, O. Harneit, Refined crystal structure of beta-uranophane, Ca(UO$_2$)$_2$(SiO$_3$OH)$_2$ · 5H$_2$O. *Am. Mineral*. **1986**, *71*, 1489.

[29] A. J. Locock, Crystal Chemistry of Uranyl Phosphates, Arsenates and Oxysalts of Chromium (V) Implications for Remediation. Thesis, University of Notre Dame, **2004**.

[30] R. J. Francis, M. J. Drewitt, P. S. Halasyamani, C. Ranganathachar, D. O'Hare, W. Clegg, S. J. Teat, Organically templated layered uranium(VI) phosphates: hydrothermal syntheses and structures of [NHEt$_3$][(UO$_2$)$_2$(PO$_4$)(HPO$_4$)] and [NPr$_4$][(UO$_2$)$_3$(PO$_4$)(HPO$_4$)$_2$]. *Chem. Commun*. **1998**, *2*, 279.

[31] J. A. Danis, W. H. Runde, B. Scott, J. Fettinger, B. Eichhorn, Hydrothermal synthesis of the first organically templated open-framework uranium phosphate. *Chem. Commun*. **2001**, *22*, 2378.

[32] M. Saadi, C. Dion, F. Abraham, Synthesis and crystal structure of the pentahydrated uranyl orthovanadate (UO$_2$)$_3$(VO$_4$)$_2$ · 5H$_2$O, precursor for the new (UO$_2$)$_3$(VO$_4$)$_2$ uranyl-vanadate. *J. Solid State Chem*. **2000**, *150*, 72.

[33] F. C. Hawthorne, D. M. C. Huminicki, The crystal chemistry of beryllium. *Rev. Mineral. Geochem*. **2002**, *50*, 333.

[34] D. M. C. Huminicki, F. C. Hawthorne, The crystal chemistry of phosphate minerals. *Rev. Mineral. Geochem*. **2002**, *48*, 123.

[35] T. H. Gier, X. Bu, G. D. Stucky, W. T. A. Harrison, Tetrahedral networks containing beryllium: Syntheses and Structures of Be$_3$(PO$_4$)$_2$ · 2H$_2$O and Be(HAsO$_4$) · H$_2$O. *J. Solid State Chem*. **1999**, *146*, 394.

[36] C. C. Pye, An ab initio study of beryllium(II) hydration. *J. Mol. Struct. THEOCHEM* **2009**, *913*, 210.

[37] W. W. Rudolph, D. Fischer, G. Irmer, C. C. Pye, Hydration of beryllium(II) in aqueous solutions of common inorganic salts. A combined vibrational spectroscopic and ab initio molecular orbital study. *Dalton Trans*. **2009**, *33*, 6513.

[38] P. B. Moore, T. Araki, I. M. Steele, G. H. Swihart, Gainesite, sodium zirconium beryllophosphate: a new mineral and its crystal structure. *Am. Mineral*. **1983**, *68*, 1022.

[39] E. E. Foord, M. E. Brownfield, F. E. Lichte, S. J. Sutley, McCrillisite, NaCs(Be,Li)Zr$_2$(PO$_4$)$_4$ · 1-2H$_2$O, a new mineral species from Mount Mica, Oxford Country, Maine, and new data for gainesite. *Can. Mineral*. **1994**, *32*, 839.

[40] W. D. Birch, A. Pring, E. E. Foord, Selwynite, NaK(Be,Al)Zr$_2$(PO$_4$)$_4$ · 2H$_2$O, a new gainesite-like mineral from Wycherproof, Victoria, Australia. *Can. Mineral*. **1995**, *33*, 55.

[41] W. Baur, T. Ohta, The Si$_5$O$_{16}$ pentamer in zunyite refined and empirical relations for individual silicon-oxygen bonds. *Acta Crystallogr. B*. **1982**, *38*, 390.

Graphical synopsis

Fabrice Dal Bo, Sergey M. Aksenov,
Frédéric Hatert and Peter C. Burns

Synthesis, IR spectroscopy and crystal structure of [(UO$_2$)$_2${Be(H$_2$O)$_2$(PO$_4$)$_2$}]·(H$_2$O), the first compound with a trimer beryllophosphate anion

Synopsis: The first uranyl beryllophosphate has been synthesized under hydrothermal method. The structure consists of sheets based on the well-known uranophane anion-topology. Unbranched [BeP$_2$O$_8$(H$_2$O)$_2$]$^{4-}$ trimer is observed for the first time in inorganic oxysalts.